IOP Conf. Series: Earth and Environmental Science **136** (2018) 012017 doi:10.1088/1755-1315/136/1/012017

Variable speed control in wells turbine-based oscillating water column devices: optimum rotational speed

J Lekube, A J Garrido and I Garrido

Automatic Control Group (ACG). Institute of Research and Development of Processes (IIDP). Department of Automatic Control and Systems Engineering, Faculty of Engineering of Bilbao, University of the Basque Country (UPV/EHU), Bilbao, Spain

E-mail: jon.lecube@ehu.eus

Abstract. The effects of climate change and global warming reveal the need to find alternative sources of clean energy. In this sense, wave energy power plants, and in particular Oscillating Water Column (OWC) devices, offer a huge potential of energy harnessing. Nevertheless, the conversion systems have not reached a commercially mature stage yet so as to compete with conventional power plants. At this point, the use of new control methods over the existing technology arises as a doable way to improve the efficiency of the system. Due to the non-uniform response that the turbine shows to the rotational speed variation, the speed control of the turbo-generator may offer a feasible solution for efficiency improvement during the energy conversion. In this context, a novel speed control approach for OWC systems is presented in this paper, demonstrating its goodness and affording promising results when particularized to the Mutriku's wave power plant.

1. Introduction

Wave energy generation potential is calculated to be 16 PWh each year, approximately 50% of energy demand by 2040. Taking this into account, current research studies are principally focused on improving the efficiency of conversion systems so as to achieve the cost-effective use of wave energy. Moreover, several countries are being supporting the development of diverse facilities along the Atlantic coasts. Among this projects stand the construction of the NEREIDA MOWC wave power plant in Mutriku – Basque Country – executed by the Basque Energy Agency (EVE) [1]. 16 Wells turbines of 18.5 kW each installed in the wave power plant generated the first GWh of cumulative wave energy supplied to the grid in January 2016 (see figure 1). Thanks to the NEREIDA wave power plant on-shore OWC devices and control strategies can be easily tested, since the aim of the power plant is not only the power generation but also to facilitate the development of the technology.

Figure 1. Turbo-generator module in NEREIDA MOWC wave power plant (Mutriku, Spain).

2. OWC Devices

OWC-based conversion systems use the airflow generated by the wave to move the turbine. In order to produce the airflow through the turbine, it is necessary a capture chamber where the air is compressed by the wave. The capture chamber consists of a square cubicle with an opening in the lower part through which the wave enters the chamber. Such opening always remains under the Still Water Level (SWL), as it can be seen in figure 2.

The turbine is placed in the upper part of the capture chamber. The air compressed within the chamber is pushed and pulled through the turbine, and thus, the bidirectional airflow makes the turbo-generator to rotate.

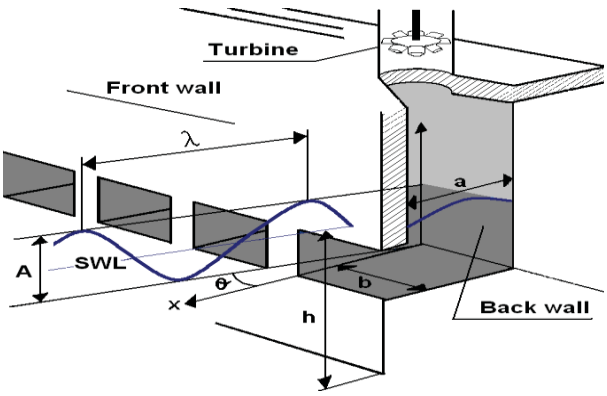

Figure 2. Oscillating Water Column system scheme.

Figure 3. Wells turbine in NEREIDA MOWC wave power plant.

In spite of the fact that new more efficient turbines, such as bi-radial turbine, are currently emerging, Wells [2-5] and impulse turbines [6] are still used in OWC devices (see figure 3). The Wells turbine is considered a self-rectifying turbine since it provides a unidirectional rotation from a bidirectional airflow, so that both incoming and outgoing wave energy can be harnessed.

3. Model statement

Although different approaches are currently available, Airy linear theory provides a proper estimation of the surface of regular waves [7]:

$$y(x,t) = a \cdot \sin\left(\frac{2\pi}{\lambda}(ct - x)\right), \tag{1}$$

where a is the wave amplitude, λ is the wavelength and c is the propagation speed.
Hence, the airflow velocity through the turbine can be obtained from the expression above as [8]

$$v_t(t) = \frac{8awc}{\pi D^2} \cdot \sin\frac{\pi l}{cT} \cos\frac{2\pi}{T} t\,, \tag{2}$$

where l is the OWC chamber length, w is the chamber width, D is the diameter of the turbine and T is the wave period.
The mechanical torque applied by the turbine in case of OWC devices can be expressed as

$$T_t = C_t \frac{\rho b l_1 n}{2} r\left(v_t^2 + (r \cdot \omega_t)^2\right), \tag{3}$$

where ρ is the air density, b is the blade span, l_1 is the blade chord, n is the number of blades, r is the tip radius, C_t is the torque coefficient and ω_t is turbine rotational speed.

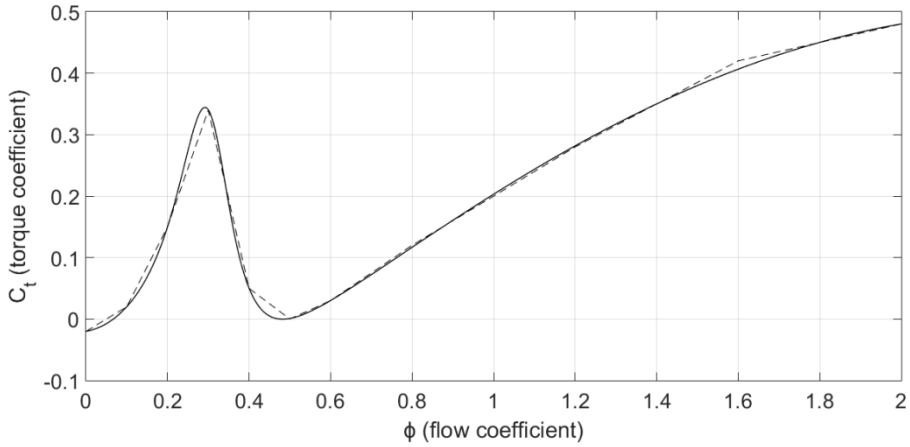

Figure 4. Torque coefficient vs. flow coefficient. Experimental (dashed) and approximated (solid) curves.

C_t is a feature of the turbine given as a characteristic curve, previously measured using empirical methods. Figure 4 shows the characteristic curve of a Wells turbine used in OWC systems, where C_t is given as a function of the flow coefficient, ϕ:

$$\phi = \frac{v_t}{r \cdot \omega_t}. \tag{4}$$

With the aim of response smoothing and an easier analytical handling of the model, C_t has been approximated to a polynomial equation where the vectors specifying the numerator and denominator coefficients are $\boldsymbol{p}$ and $\boldsymbol{q}$, respectively:

$$C_t = \frac{\sum_{i=0}^{6} p_i \cdot \phi^{i-1}}{\sum_{i=0}^{4} q_i \cdot \phi^{i-1}}, \tag{5}$$

where, according to the turbine of figure 3, elements of $\boldsymbol{p}$ vector are $p_1 = -0.001398$, $p_2 = 0.01456$, $p_3 = 0.1408$, $p_4 = -0.7687$, $p_5 = 0.9818$, $p_6 = -0.202$, whereas $\boldsymbol{q}$ vector is composed by $q_1 = -0.06988$, $q_2 = -0.3182$, $q_3 = 0.06089$, $q_4 = 1$.
It must be reasonably assumed that ϕ must be less than 0.3. Otherwise, stalling behavior appears in the turbine dynamics that makes the efficiency of the system to drop. Therefore, according to equation (4), there must be a minimum rotational speed for each airflow velocity. The current control systems used in OWC devices limit the airflow velocity using a damper when the turbo-generator is not able to reach the minimum rotational speed to avoid stalling [9-14]. However, using speed control the stalling avoidance can be addressed by speeding up the generator until the minimum rotational speed [15-20]. This solution may offer a faster response than the mechanical system of the damper. In order to improve the system response different control method approaches may be used [21-28].

4. Optimum rotational speed

Apart from the stalling behaviour avoidance, the efficiency of the system may be further improved by setting a proper rotational speed of the turbine.
The efficiency of the turbo-generator system, which is composed by Wells turbine directly related to C_t, varies depending on the rotational speed of the turbine. That means that there exists an optimum rotational speed where the power applied by the turbine is maximized. The search of the optimum operating point can be achieved by means of the Maximum Power Point Tracking (MPPT) method. MPPT has been successfully implemented in wind energy and photovoltaic solar plants.

Table 1. Airflow speed and rotational speed vs. wave amplitude and period.

State	a (m)	T (s)	v_t (m/s)	ω_{opt} (rad/s)	ω_{min} (rad/s)
1	1	12	22.835	500.04	202.97
2	0.7	12	15.984	350.03	142.08
3	0.9	11	22.401	490.55	199.12
4	0.8	10	21.879	479.13	194.49
5	0.6	10	16.409	359.35	145.86
6	0.6	9	18.206	398.69	161.83
7	0.6	8	20.440	447.61	181.69
8	0.4	8	13.637	298.41	121.13
9	0.4	7	15.527	340.02	138.02

In this context, figure 5 shows the mechanical power developed by the turbine according to the airflow velocity from equation (2) produced by different sea states in table 1. The parameters of each sea condition have been summarized in table 1, whereas the features of the OWC capture chamber and the turbine have been taken from Mutriku wave power plant, as summarized in table 2. As it can be seen in figure 5, the mechanical power applied in the turbo-generator shaft is maximized at a particular rotational speed for each sea condition. The discontinuous line represents the corresponding MPPT curve defined, and it may be approximated as:

$$P_{\max} = K \cdot \omega_t^3, \tag{6}$$

being $K = C_{t,opt} \frac{\rho l_1 bn}{2} r^3 \left(\phi_{opt}^2 + 1\right)$, where ϕ_{opt} is the value of the flow coefficient at optimum point and $C_{t,opt}$ is the value of C_t according to equation (5) and ϕ_{opt}.

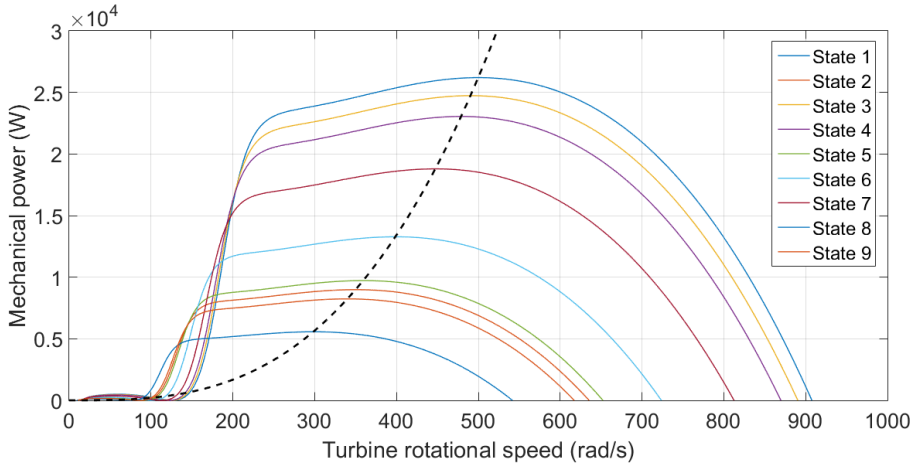

Figure 5. Mechanical power vs. turbine rotational speed for different sea states. Maximum power point curve (dashed).

Table 2. OWC chamber and Wells turbine parameters for Mutriku MOWC power plant.

ρ	Air density	1.19 kg·m^{-3}
w	Chamber width	4.5 m
l	Chamber length	4.3 m
b	Blade span	0.21 m
l_1	Blade chord	0.165 m
r	Turbine's tip radius	0.375 m
n	Number of blades	5

5. Control statement and simulation

In order to set the optimum rotational speed of the turbine, the turbo-generator must operate at variable speed mode. In this sense, the Doubly-Fed Induction Generator (DFIG) has been chosen to achieve the control objectives pursued in this paper [29-31].
Figure 6 shows an integrated complete wave-to-wire control scheme implemented over the plant.

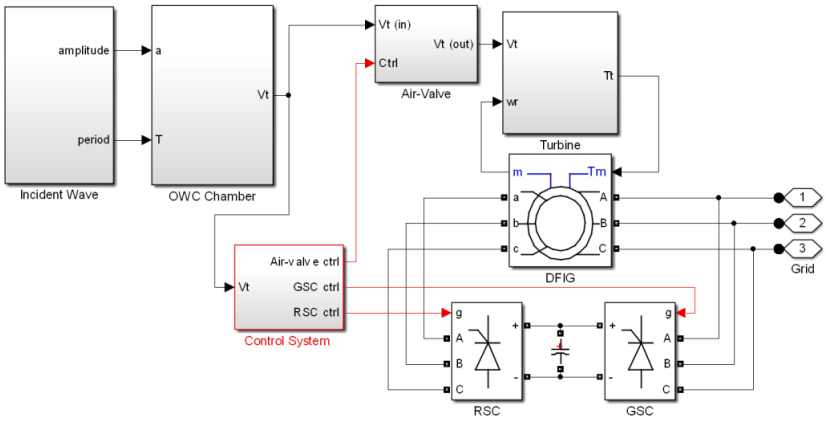

Figure 6. Full wave-to-wire model used in simulations.

The control system in figure 6 is responsible for establishing the control signals in the DFIG converters so as to set the slip of the turbo-generator and to keep the optimum rotational speed during the power conversion. The optimum rotational speed is determined taking all the information in the previous section into account, and in particular considering the condition in equation (6).

Three illustrative case studies have been carried out so as to test the goodness of the proposed control method. The first case study considers a system without speed control. The second case study implements the speed control to avoid the stalling behavior. That is to say, the control system ensures that a minimum rotational speed is reached by the turbo-generator for stalling avoidance. Finally, in the third case study the MPPT strategy is implemented by setting the optimum rotational speed by means of variable speed control.

In order to carry out the illustrative case studies mentioned above, regular waves have been considered taking into account amplitudes and periods measured in NEREIDA MOWC power plant. In particular, the values correspond to May 12, 2014, 02.00 am. Figure 7 shows such amplitudes and periods of regular waves.

The rotational speeds reached by the turbo-generator during the simulation are shown in figure 8. As it can be seen, the rotational speed does not show large variations for the uncontrolled plant, whereas the MPPT method not only requires higher rotational speeds but also an accurate control over the slip of the generator so as to reach fast variations. In the same way, the electric power generated in different case studies is shown in figure 9. It can be easily deduced that the use of variable speed control, and in particular the MPPT control method by means of an optimum rotational speed setting, allows more efficient energy harnessing.

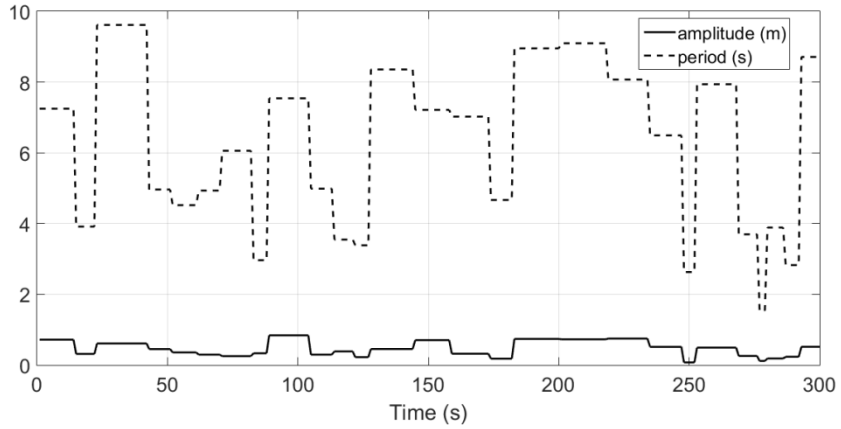

Figure 7. Amplitudes and periods of waves used in simulations.

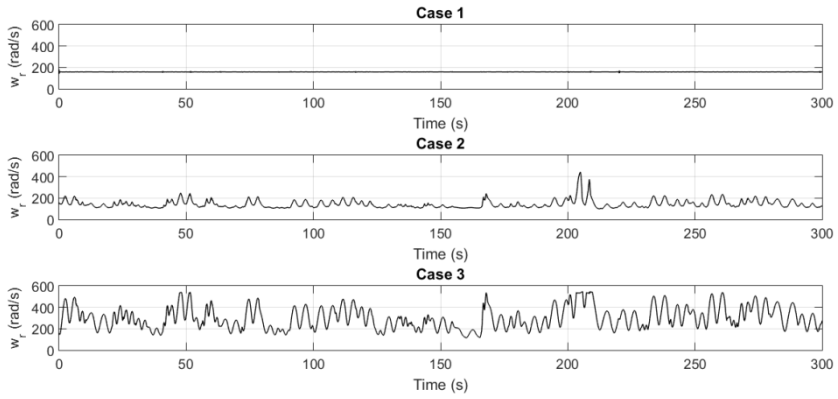

Figure 8. Turbine rotational speeds. Case 1: uncontrolled plant. Case 2: speed control for stalling avoidance. Case 3: speed control with MPPT.

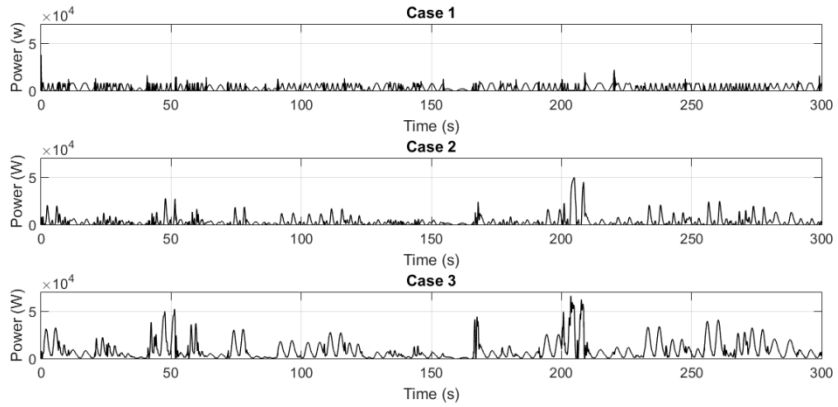

Figure 9. Output electric power of the turbo-generator. Case 1: uncontrolled plant. Case 2: speed control for stalling avoidance. Case 3: speed control with MPPT.

6. Conclusion

A variable speed control can be developed for OWC-based systems. In this sense, an optimum rotational speed can be set using MPPT control method so as to maximize the output power. Besides, a full wave-to-wire model has been implemented using experimental data from Mutriku wave power plant, one of the OWC facilities currently in operation. The simulations not only demonstrate that the use of variable speed control may considerably improve the efficiency of OWC systems, but also an implementation of MPPT control method has been successfully simulated for OWC devices with promising results.

7. References

[1] Torre-Enciso Y 2009 Mutriku Wave Power Plant: From Conception to Reality *European Federation of Agencies and Regions for Energy and the Environment (FEDARENE)* Brussels, Belgium

[2] Gato L M C, Warfield V and Thakker A 1996 Performance of a high-solidity wells turbine for an OWC wave power plant *Journal of Energy Resources Technology* **118(4)** pp 263–268

[3] Inoue M, Kaneko K, Setoguchi T and Saruwatari T 1988 Studies on the Wells turbine for wave power generator (turbine characteristics and design parameter for irregular wave) *JSME International Journal* **31(4)** pp 676–682

[4] Setoguchi T and Takao M 2006 Current status of self rectifying air turbines for wave energy conversion *Energy Conversion and Management* **47(15/16)** pp 2382–2396

[5] Raghunathan S 1985 Performance of the Wells self-rectifying turbine *Aeronautical Journal* **89(1369)** pp 369–379
[6] Jayashankar V, Anand S, Geetha T, Santhakumar S, Jagadeesh Kumar V, Ravindran M, Setoguchi T, Takao M, Toyota K and Nagata S 2009 A twin unidirectional impulse turbine topology for OWC based wave energy plants *Renewable Energy* **34(3)** pp 692–698
[7] Le Roux J P 2008 An extension of the Airy theory for linear waves into shallow water *Coastal Engineering* **55(4)** pp 295–301
[8] Garrido A J, Otaola E, Garrido I, Lekube J, Maseda F J, Liria P and Mader J 2015 Mathematical Modeling of Oscillating Water Columns Wave-Structure Interaction in Ocean Energy Plants *Mathematical Problems in Engineering* **2015** Article ID 727982
[9] Ormaza M A, Goitia M A, Hernández A J G and Hernández I G 2009 Neural control of the Wells turbine-generator module *Proceedings of the IEEE Conference on Decision and Control* Shanghai China pp 7315–7320
[10] Garrido A J, Garrido I, Alberdi M, Amundarain M, Barambones O and Romero J A 2013 Robust control of oscillating water column(OWC) devices: power generation improvement *MTS/IEEE Proceedings of the OCEANS—San Diego* San Diego California USA pp 1–4 Article ID 6740982
[11] Sameti M and Farahi E 2014 Output power for an oscillating water column wave energy convertion device *Ocean and Environmental Fluid Research* **1(2)** pp 27–34
[12] El Marjani A, Castro Ruiz F, Rodriguez M A and Parra Santos M T 2008 Numerical modelling in wave energy conversion systems *Energy* **33(8)** pp 1246–1253
[13] Garrido A J, Garrido I, Amundarain M, Alberdi M and De la Sen M 2012 Sliding-mode control of wave power generation plants *IEEE Transactions on Industry Applications* **48(6)** pp 2372–2381 DOI 10.1109/TIA.2012.2227096
[14] Falcao A F D O, Vieira L C, Justino P A P and André J M C S 2003 By-pass air-valve control of an OWC wave power plant *Journal of Offshore Mechanics and Arctic Engineering* **125(3)** pp 205–210
[15] Garcia-Rosa P B, Cunha J P V S, Lizarralde F, Estefen S F and Costa P R 2009 Efficiency optimization in a wave energy hyperbaric converter *International conference on Clean Electrical Power*
[16] Amon A, Brekken K A and Schacher A 2012 Maximum Power Point Tracking for Ocean Wave Energy Conversion *IEEE Transactions on Industry Applications* **48(3)** pp 1079-1086
[17] Zou Y, Elbuluk M E and Sozer Y 2013 Stability analysis of Maximum Power Point Tracking (MPPT) method in wind power systems *IEEE Transactions on Industry Applications* **49(3)** pp 1129-1136
[18] Pucci M and Cirrincione M 2011 Neural MPPT control of wind generators with induction machines without speed sensors *IEEE Transactions on Industrial Electronics* **58(1)** pp 37-47
[19] Jayashankar V, Udayakumar K, Karthikeyan B, Manivannan K, Venkatraman N and Rangaprasad S 2000 Maximizing power output from a wave energy plant *Proc. IEEE Power Engineering Society* **3** pp 1796–1801
[20] Falcao A F D O 2002 Control of an oscillating-water-column wave power plant for maximum energy production *Applied Ocean Research* **24** pp 73-82
[21] Garrido A J, De La Sen M, Soto J C, Barambones O and Garrido I 2008 Suboptimal regulation of a class of bilinear interconnected systems with finite-time sliding planning horizons *Mathematical Problems in Engineering* **2008** Article ID 817063 DOI 10.1155/2008/817063
[22] Barambones O and Garrido A J 2007 An adaptive variable structure control law for sensorless induction motors *European Journal of Control* **13** pp 382-392
[23] Liu X and Kong X 2013 Nonlinear Model Predictive Control for DFIG-Based Wind Power Generation *IEEE Transactions on Automation Science and Engineering* **11(4)** pp 1046-1055
[24] Sevillano M G, Garrido I and Garrido A J 2012 Sliding-mode loop voltage control using ASTRA-Matlab integration in Tokamak reactors *International Journal of Innovative Computing, Information and Control* **8(9)** pp 6473-6489

[25] Alkorta P, Barambones O, Garrido A J and Garrido I 2007 SVPWM variable structure control of induction motor drives *IEEE International Symposium on Industrial Electronics* pp 1195-1200 Article ID 4374768 DOI 10.1109/ISIE.2007.4374768
[26] Sevillano M G, Garrido I and Garrido A J 2011 Control-oriented Automatic System for Transport Analysis (ASTRA)-Matlab integration for Tokamaks *Energy* **36(5)** pp 2812-2819 DOI 10.1016/j.energy.2011.02.022
[27] De La Sen M, Abbas M and Saleem N 2017 On Optimal Fuzzy Best Proximity Coincidence Points of Proximal Contractions Involving Cyclic Mappings in Non-Archimedean Fuzzy Metric Spaces *Mathematics* **5(22)** DOI 10.3390/math5020022
[28] De La Sen M, Hedayati V, Gholizade Y and Rezapour S 2017 The existence and numerical solution for a k-dimensional system of multi-term fractional integro-differential equations *Nonlinear Analysis: Modelling and Control* **22(2)** pp 188-209
[29] Iwanski G and Koczara W 2008 The DFIG-based power generation system with UPS function for variable-speed applications *IEEE Transactions on Industrial Electronics* **55(8)** pp 3047–3054
[30] Hu J, He Y, Xu L and Williams B W 2009 Improved control of DFIG systems during network unbalance using PI–R current regulators *IEEE Transactions on Industrial Electronics* **56(2)** pp 439–451
[31] Garrido I, Garrido A J, Alberdi M, Amundarain M and Barambones O 2013 Performance of an ocean energy conversion system with DFIG sensorless control *Mathematical Problems in Engineering* **2013** Article ID 260514 DOI 10.1155/2013/260514

Acknowledgments
This work was supported in part by the University of the Basque Country (Universidad del País Vasco UPV/Euskal Herriko Unibertsitatea EHU) through Project PPG17/33 and by the MINECO through the Research Project DPI2015-70075-R (MINECO/FEDER, EU), as well as to the Basque Government through Ph.D. Grant PIF PRE_2016_2_0193.
The authors would like to thank the collaboration of the Basque Energy Agency (EVE) through Agreement UPV/EHUEVE23/6/2011, the Spanish National Fusion Laboratory (EURATOM-CIEMAT) through Agreement UPV/EHUCIEMAT08/190 and EUSKAMPUS – Campus of International Excellence. They would also like to thank Yago Torre-Enciso and Olatz Ajuria from EVE for their collaboration and help.